# Hydrothermal Synthesis of Nanostructured Vanadium Oxides

Jacques Livage

*Materials* **2010**, *3*, 4175-4195; doi:10.3390/ma3084175

OPEN ACCESS

*materials*

**ISSN 1996-1944**

www.mdpi.com/journal/materials

*Review*

# Hydrothermal Synthesis of Nanostructured Vanadium Oxides

**Jacques Livage**

Chimie de la Matière Condensée, Collège de France, 11 place Marcelin Berthelot, 75231 Paris, France; E-Mail: jacques.livage@upmc.fr; Tel.: 33 (0)1 44 27 15 00; Fax: 33 (0)1 44 27 15 04

*Received: 1 July 2010; in revised form: 27 July 2010 / Accepted: 30 July 2010 / Published: 2 August 2010*

**Abstract:** A wide range of vanadium oxides have been obtained via the hydrothermal treatment of aqueous V(V) solutions. They exhibit a large variety of nanostructures ranging from molecular clusters to 1D and 2D layered compounds. Nanotubes are obtained via a self-rolling process while amazing morphologies such as nano-spheres, nano-flowers and even nano-urchins are formed via the self-assembling of nano-particles. This paper provides some correlation between the molecular structure of precursors in the solution and the nanostructure of the solid phases obtained by hydrothermal treatment.

**Keywords:** vanadium oxide; nanostructure; aqueous chemistry

## 1. Introduction

The properties of solid state materials mainly depend on their structure and morphology. Therefore nanostructured materials are becoming very popular. They offer a great potential for improving properties and find applications in many fields such as microelectronics, batteries, sensing devices, nanoprobes and even nanomedicine [1-4]. Many nanostructured materials have been described during the past few years. Among them nanostructured vanadium oxides have been extensively studied since the discovery of VOx nanotubes by R. Nesper and his group [5,6]. They exhibit a great variety of nanostructures, ranging from 1D to 3D [7] and $V_2O_5$ has even been chosen as a model system for the description of nanostructured materials. Vanadium oxides find major applications in the field of lithium ion batteries [8-11].

One of the main points for a real development of nanostructured materials would be a better understanding of their formation in order to be able to build taylor-made nanostructures. The usual solid state synthesis of vanadium pentoxide via the thermal decomposition of ammonium

metavanadate leads to the well known orthorhombic oxide $\alpha$-$V_2O_5$ that exhibits a layered structure made of edge and corner sharing [$VO_5$] double chains [12]. Many other structures based on vanadium oxide have been described in the literature [13,14]. Different types of vanadium coordination polyhedra such as trigonal bipyramids to square pyramids and tetrahedra are observed. Moreover, $V^{5+}$ can be easily reduced leading to mixed valence vanadium oxides in which both $V^{5+}$ and $V^{4+}$ and even $V^{3+}$ ions are observed. Therefore a large variety of crystalline vanadium oxides have been described. They are usually synthesized via the hydrothermal heating of aqueous solutions [15]. Nanostructured vanadium oxides exhibit unusual morphologies such as nanowires, nanobelts, nanorods, nanotubes and even flower-like or nano-urchin shapes [4-11]. This paper discusses the chemical parameters that are responsible for the formation of a vanadium oxide network from V(V) precursors in aqueous solutions. The molecular structure of these precursors mainly depends on pH but the way they self-assemble depends on the nature of other species in the solution. Supramolecular associations are formed leading to a large variety of crystalline phases. The structure and properties of these nanostructured vanadium oxides have been widely described but the chemical mechanisms leading to their formation from aqueous solutions remain largely unknown. In this paper we would like to draw some relationships between the structure of molecular precursors in aqueous solutions and the nanostructure of vanadium oxides obtained after hydrothermal treatment. This would show how the aqueous chemistry of V(V) can be controlled in order to make nanostructured vanadium oxides, providing an overview of most recent results obtained during the past decade.

## 2. Vanadium (V) Species in Aqueous Solutions

The aqueous chemistry of V(V) has been extensively studied and a large variety of molecular species have been described [16]. At room temperature, they mainly depend on vanadium concentration and pH (Figure1). Two basic reactions, hydrolysis and condensation, occur when vanadium salt is dissolved in water.

**Figure 1.** V(V) solute species in aqueous solutions as a function of pH and concentration.

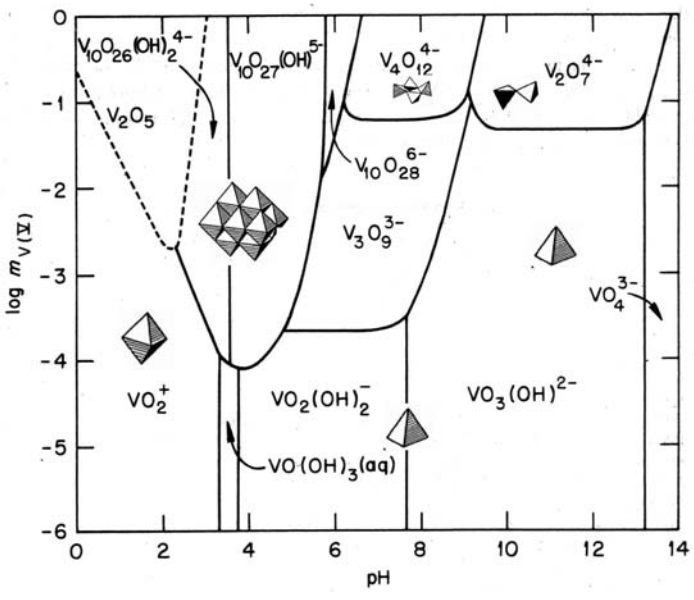

### *2.1. Hydrolysis*

In aqueous solutions, $V^{5+}$ ions are solvated by dipolar water molecules giving hydrated $[V(OH_2)_n]^{5+}$ species. However, because of the strong polarizing power of the small and highly charged $V^{5+}$ ion, coordinated water molecules are partially deprotonated and the solution becomes more acidic. This hydrolysis reaction can be described as follows:

$$[V(OH_2)_6]^{5+} + hH_2O \Rightarrow [V(OH)_h(OH_2)_{6-h}]^{(5-h)+} + hH_3O^+$$

The hydrolysis ratio 'h' increases with pH leading to the formation of aquo, hydroxo and oxo species. It can be easily predicted in the frame of the so-called 'partial charge model' based on the electronegativity equalization principle of R.T. Sanderson [17-18]. According to this model, we may assume that an equilibrium is reached when the mean electronegativity $\chi_p$ of hydrolyzed vanadium precursors $[V(OH)_h(OH_2)_{6-h}]^{(5-h)+}$ becomes equal to the mean electronegativity $\chi_{aq}$ of the aqueous solution. In such solutions, protons are delocalized over the whole network of hydrogen bonds. As a result the electronegativity of solvated protons becomes equal to that of bulk water molecules and the electronegativity of aqueous solutions changes with pH. It decreases linearly with pH as follows:

$$\chi_{aq} = \chi_{aq}^{\ 0} - \lambda pH$$

This leads to the following expression [18]:

$$\chi_{aq} = 2.732 - 0.035pH$$

The mean electronegativity of an aqueous solution decreases linearly with pH from 2.732 at pH 0 down to 2.242 at pH 14 while the hydrolysis ration increases from h = 4.5 $[VO_2(OH_2)_4]^+$ to h = 6.2 $[VO_3(OH)]^{2-}$ (Figure 2).

**Figure 2.** Hydrolysis ratio 'h' of V(V) precursors $[V(OH)_h(OH_2)_{6-h}]^{(5-h)+}$ as a function of pH.

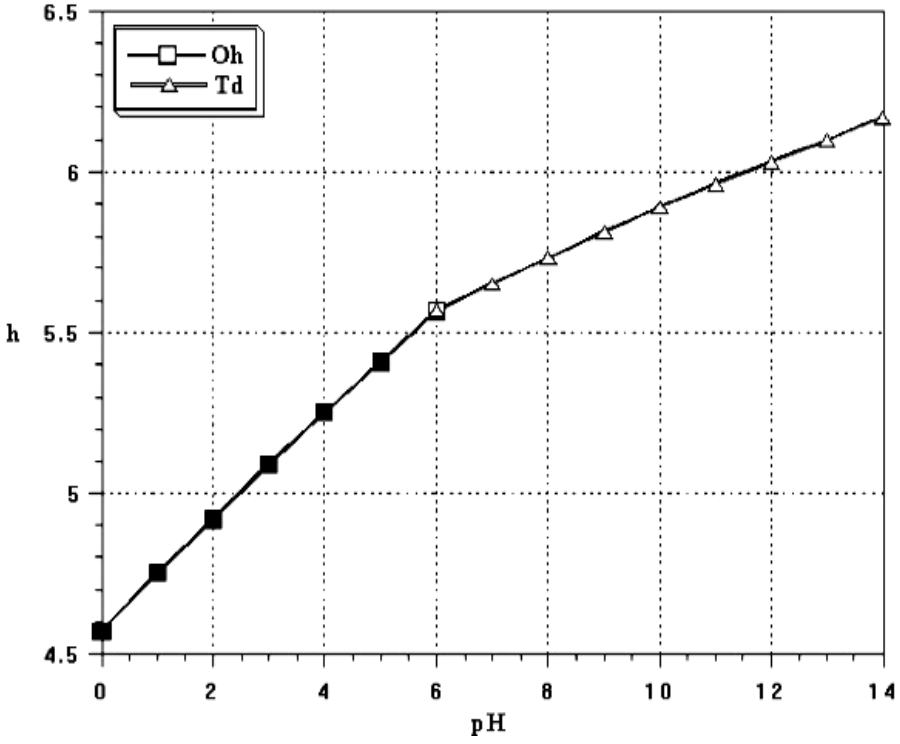

At low pH (pH < 2), the Partial Charge Model gives an hydrolysis ratio h = 4 and the $V^V$ precursor should correspond to $[V(OH)_4(OH_2)_2]^+$. However, some internal proton transfer occurs between V-OH groups in order to decrease the positive charge of vanadium. This leads to the formation of vanadyl cations $[VO_2(OH_2)_4]^+$ or $[VO_2]^+$ in which two V = O double bonds are formed in cis positions [20].

The coordination number of V(V) decreases from 6 to 4 above pH ≈ 6. Actually the 'σ' electron transfer from the coordinated water molecules toward the empty d orbitals of $V^{5+}$ ions increases with deprotonation and the positive partial charge of vanadium decreases. V-O bonds become more covalent and vanadium coordination decreases leading to four-fold coordinated vanadate species $[H_nVO_4]^{(3-n)-}$. This coordination change can be easily seen with the naked eyes. The color of $V^{5+}$ ($3d^0$) ions is due to electron transfers from the oxygen bonding orbitals to the empty vanadium 'd' orbitals. These charge transfer bands move toward UV when the crystal field splitting of 'd' orbitals decreases. Six-fold coordinated V(V) decavanadate solutions are typically orange whereas four-fold coordinated metavanadates are colorless **[**19**]**.

Tetrahedral species $[H_nVO_4]^{(3-n)-}$ are then formed. They are progressively deprotonated as pH increases leading to $[VO_4]^{3-}$ species above pH 12.

### *2.2. Condensation*

Actually, monomeric species are only observed in very dilute solutions. Condensation occurs at higher vanadium concentration (Figure1). Two main reactions are involved in this condensation process.

$$\text{Olation} \rightarrow \text{-V-OH + -V-OH}_2 \Rightarrow \text{-V-OH-V- + H}_2\text{O}$$
$$\text{Oxolation} \rightarrow \text{-V-OH + HO-V- } \Rightarrow \text{ -V-O-V- + H}_2\text{O}$$

They both involve the nucleophilic addition of negatively charged $OH^{\delta-}$ groups onto positive vanadium cations $V^{\delta+}$. Hydroxo V-OH groups are then required for condensation to occur, but olation reactions, in which labile water molecules are already formed, are kinetically faster than oxolation.

At low pH, vanadyl precursors $[VO_2]^+$ cannot lead to condensed species and anions have to be added for precipitation to occur. Vanadyl phosphates $VOHPO_4.nH_2O$, for instance, can be obtained in which $[VO_2]^+$ cations are surrounded by phosphate anions, V-O-V bonds are not formed [21].

The precipitation of vanadium pentoxide $V_2O_5$ occurs at the Point of Zero Charge (PZC), around pH ≈ 2. It should arise from the polycondensation of the neutral precursor $[VO(OH)_3(OH_2)_2]^0$. According to its molecular structure, condensation is not possible along the *z* direction O=V-$OH_2$. It occurs only within the *xy* plane where V-OH bonds are present (Figure 3). Fast olation reactions along the *x* axis, $H_2O$-V-OH lead to chains of edge sharing $[VO_5]$ square pyramids. These chains are then linked via oxolation reactions along the *y* axis HO-V-OH, leading to vanadium oxide layers made of corner sharing double chains as in orthorhombic $V_2O_5$. This two step mechanism may explain the ribbon-like structure of vanadium oxide gels $V_2O_5.nH_2O$ that have been described as $V_2O_5$ bi-layers made of square pyramidal $[VO_5]$ units with intercalated water molecules [22-25].

Negatively charged decavanadate clusters $[H_nV_{10}O_{28}]^{(6-n)-}$, made of 10 edge-sharing $[VO_6]$ octahedra, are formed above pH 2. Small and highly charged $V^{5+}$ ions polarize terminal $O^{2-}$ ligands resulting in closed clusters in which M=O bonds point radially toward the outside. Decavanadates

behave as strong acids and further condensation does not occur under ambiant conditions. Polyvanadate solid phases are precipitated in the presence of cations. They are built of decavanadate anionic clusters separated by cations [26].

**Figure 3.** Molecular structure of $V^V$ precursors in the pH range 2-8.

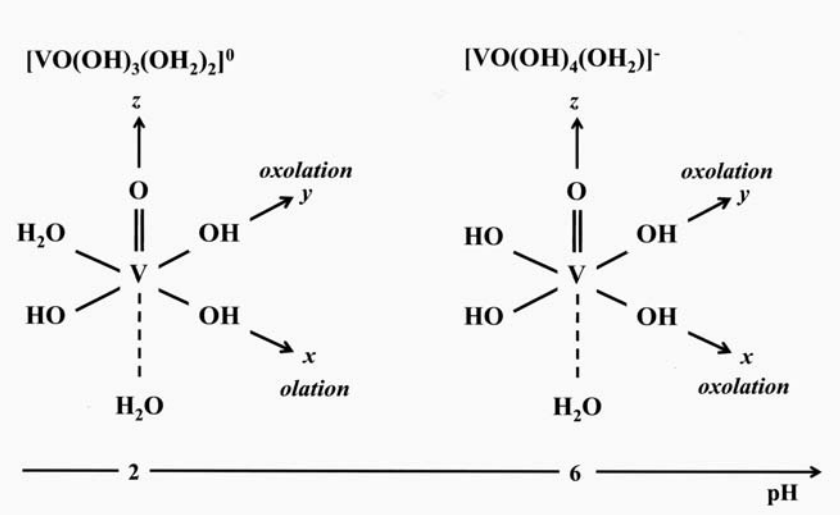


Vanadium coordination decreases above pH ≈ 6 giving tetrahedral anionic precursors $[H_nVO_4]^{(3-n)-}$. In the pH range 6–9, difunctional precursors $[H_2VO_4]^-$ lead to condensed metavanadates forming cycles or chains. Cyclic species such as $[V_4O_{12}]^{4-}$ are usually observed in the solution where they can be evidenced by $^{51}V$ and $^{17}O$ NMR [27], whereas chain metavanadates are currently formed in the solid state. They are built up of single chains of corner-sharing $[VO_4]$ tetrahedra as in $KVO_3$ or double chains of edge-sharing $[VO_5]$ trigonal bipyramids as in $KVO_3{\cdot}H_2O$. Their formation from cyclic $[H_nV_4O_{12}]^{(3-n)-}$ solute precursors can be described via a ring opening polymerization mechanism. The metavanadate salt of ter-butylammonium is especially interesting. Depending on temperature, both cyclic $[(CH_3)_3CNH_3]_4[V_4O_{12}]$ and chain $[(CH_3)_3CNH_3][VO_3]$ metavanadates can be synthesized from aqueous solutions. This is the first example of a solid polyoxovanadate precipitated from an aqueous solution containing discrete non protonated $[V_4O_{12}]^{4-}$ cyclic anions. A phase transition from cycles to chains can even be observed in the solid state [28].

Further deprotonation leads to $[HVO_4]^{2-}$ precursors above pH 9. The condensation of these monofunctional species is then limited to dimeric pyrovanadates $[V_2O_7]^{4-}$ made of two corner-sharing tetrahedra. Fully deprotonated oxo-anions $[VO_4]^{3-}$ in which $V^V$ is surrounded by four equivalent oxygen atoms are observed at very high pH (h = 14). There is no functional V–OH group and V–O–V bonds cannot be formed. Only orthovanadates made of isolated $[VO_4]$ tetrahedra can be obtained above pH ≈ 12.

### *2.3. Evolution of molecular precursors upon heating*

At room temperature there is a straight correlation between the molecular structure of vanadate precursors in the solution and vanadate anions in the solid precipitate. This is no longer the case when syntheses are performed under hydrothermal conditions. Adding tetramethyl ammonium $N(CH_3)_4OH$

(TMAOH) to an aqueous solution of decavanadic acid for instance leads to the precipitation of $(TMA)_4[H_2V_{10}O_{28}]$ made of anionic decavanadate clusters and $(TMA)^+$ cations while a layered compound $TMA[V_4O_{10}]$ is obtained, from the same solution, after hydrothermal heating at 180 °C (Figure 4). In both cases, the pH of the solution is the same [15].

**Figure 4.** Structure of (a) $(TMA)_4[H_2V_{10}O_{28}]$ synthesized at room temperature and (b) $TMA[V_4O_{10}]$ obtained under hydrothermal conditions.

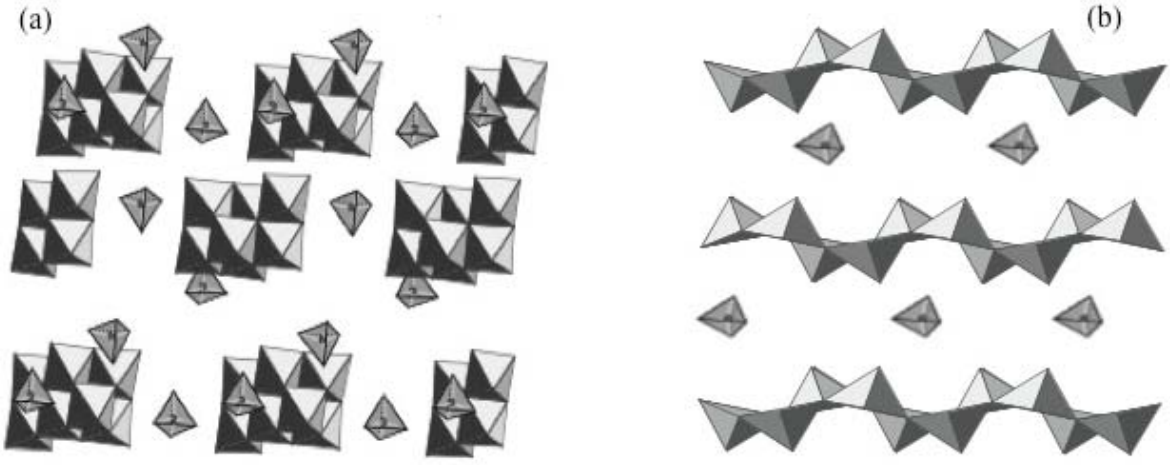


These experiments suggest that the molecular structure of V(V) precursors in aqueous solutions does not depend only on pH, but also on temperature. $^{51}V$ NMR experiments, performed at different temperatures, show that decavanadate solutions progressively transform into cyclic metavanadates $[V_4O_{12}]^{4-}$ upon heating [29]. Only metavanadates are observed around 200 °C (Figure 5). Deprotonation occurs upon heating, leading to the dissociation of decavanadates into metavanadates as follows:

$$2[H_2V_{10}O_{28}]^{6-} + 4H_2O \Rightarrow 5[V_4O_{12}]^{4-} + 12H^+$$

This reaction is reversible and decavanadates are again observed when decreasing temperature.

In dilute solutions, where only monomolecular species are formed, we may then assume that the deprotonation of the neutral precursor $[VO(OH)_3(OH_2)_5]^0$ leads to anionic species such as $[VO(OH)_4(H_2O)]^-$ that upon dehydration would give more or less protonated tetrahedral vanadate anions $[H_nVO_4]^{(3-n)-}$.

$$[VO(OH)_3(OH_2)_2]^0 \Leftrightarrow [VO(OH)_4(H_2O)]^- \Leftrightarrow [H_nVO_4]^{(3-n)-}$$

We could then suggest that upon hydrothermal treatment, solid phases built of $[VO_5]$ polyhedra are formed via the polycondensation of the intermediate molecular precursor $[VO(OH)_4(H_2O)]^-$. Its molecular structure shows that oxolation reactions only occur in the '*xy*' plane, along the four V-OH bonds leading to 2D layered compounds rather than ribbon-like particles [Figure 4].

**Figure 5.** $^{51}V$ NMR spectra of a vanadate solution recorded at different temperatures: $V_{10} = [H_2V_{10}O_{28}]^{4-}$, $V_4 = [V_4O_{12}]^{4-}$.

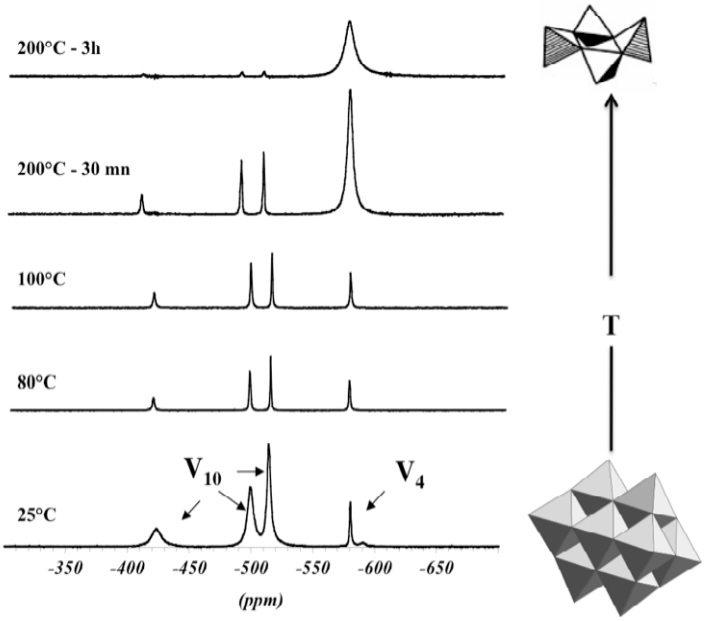


Reduction should also play a role during the thermal transformation of tetramethyl ammonium decavanadates into the layered $TMA[V_4O_{10}]$ oxide [29,30]. Such a transformation is not observed with the inorganic sodium decavanadate. Heating sodium decavanadate directly leads to the stable oxide phases $NaVO_3$ and $NaV_3O_8$. The transformation of $(TMA)_4[H_2V_{10}O_{28}].4H_2O$ into $TMA[V_4O_{10}]$ seems to occur only in the presence of organic cations. ESR experiments show that the transformation does not occur until some $V^{5+}$ are reduced into $V^{4+}$. This reduction, due to the partial decomposition of organic species, favors condensation and coordination expansion, $V^{4+}$ ions being larger than $V^{5+}$ do not adopt tetrahedral coordination.

## 3. Mixed Valence Polyoxovanadate Molecular Clusters

In the previous examples, the formation of polyoxovanadates is governed by the condensation of inorganic precursors. Cations just behave as counter ions in order to get a neutral solid network. Surprisingly foreign anionic species may also behave as templates during the formation of polyoxovanadates. The hydrothermal treatment of $V_2O_5$ and TMAOH leads to the layered compound $TMA[V_4O_{10}]$ but, in the same experimental conditions (temperature and pH), 3D crystals of $(TMA)_6[V_{15}O_{36}Cl].4H_2O$ or $(TMA)_{10}[H_3V_{18}O_{42}I].3H_2O$ are obtained in the presence of $X^-$ anions (X = Cl, I) [19]. They contain anionic clusters $[V_{15}O_{36}Cl]^{6-}$ and $[H_3V_{18}O4_2I]^{10-}$ made of $[VO_5]$ pyramids linked together to build a hollow cage. The foreign anion is trapped inside this anionic cage whose size depends on the size of the anionic species as shown by the following examples : $[CH_3CN(V_{12}O_{32}]^{4-}$, $[V_{15}O_{36}Cl]^{6-}$, $[V_{16}O_{38}Cl]^{8-}$, $[H_3V_{18}O_{42}I]^{10-}$ and $[HV_{22}O_{54}(ClO_4)]^{6-}$ [31-33].

The shape of the polyoxovanadate cages also depends on the shape of the anion. $(ClO_4)^-$ leads to the formation of spherical cages such as $[HV_{22}O_{54}(ClO_4)]^{6-}$ while elongated azide anions $(N_3)^-$ lead to ellipsoidal $[H_2V_{18}O_{44}(N_3)]^{5-}$ cluster cages [34]. The mixed valence polyoxovanadate $[V_{34}O_{82}]^{10-}$

exhibits quite a strange molecular structure. It is made of an ellipsoid-shaped $[V_{30}O_{74}]$ sheath built of 30 tetragonal $[VO_5]$ pyramids surrounding a central $[(V_4O_4)O_4]$ cube [35].

These polyoxvanadate cages can be viewed as sections of layers of vanadium pentoxide $V_2O_5$. The condensation of V–OH groups in the equatorial plane of the $[VO(OH)_4(OH_2)]^-$ precursor leads to the formation of 2D compounds made of corner and edge-sharing $[VO_5]$ pyramids. However, the way these pyramids are linked together depends on the nature of the other ionic species in the solution [36].

Large and weakly polarizing tetramethyl cations interact weakly with the negative oxygen of terminal $V = O^{\delta-}$. They only behave as counter cations in order to form a neutral solid with the anionic polyoxovanadate network. Interactions between adjacent V = O dipoles lead to a layered structure with $[VO_5]$ pyramids alternatively ‘‘up’’ and ‘‘down’’.

This is no longer the case with smaller and more polarizing inorganic anions ($Cl^-$, $I^-$, $NO_3^-$,...). The specific role of these anions should be due to the particular geometry of $[VO_5]$ pyramids in which the weakly bonded water molecule $V\text{-}OH_2$ opposite to the V = O bond is highly labile. Negative anions $X^-$ can then interact with the positive $V^5$ along the *z* axis, leading to the curved condensation of $[VO_5]$ square pyramids around this central anion to form a closed cage [37,38]. All V = O dipoles are then oriented toward the outside of the shell where they repeal each other, leading to the formation of convex surfaces (Figure 6). Interactions between the central anion and the negatively charged polyoxovanadate cage are very weak. The vanadate cage is mainly polarized by the central anion so that the negative density is pushed toward the V = O pointing outside of the cage where they interact with the positive cations [39].

**Figure 6.** Polyoxovanadate clusters formed in the presence of $X^-$ anions $[V_{15}O_{36}Cl]^{6-}$ and $[H_3V_{18}O_{42}I]^{10-}$.

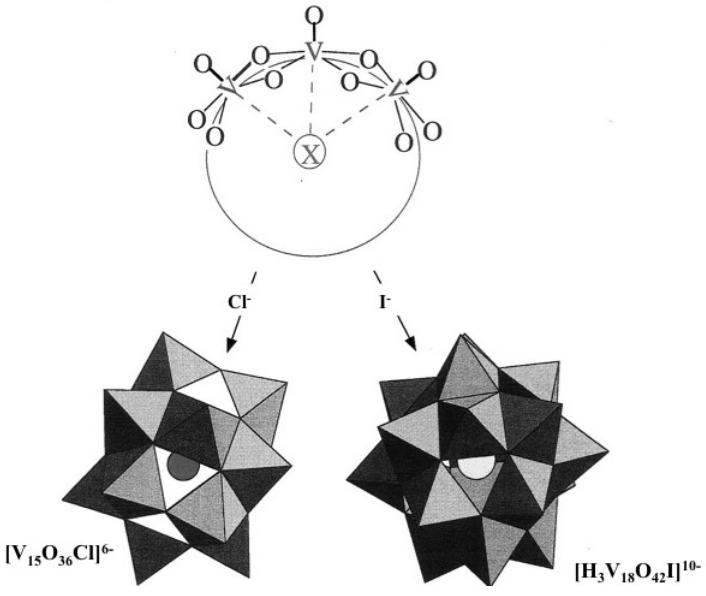


## 4. Nanostructured Vanadium Oxides

### *4.1. From 1D to 2D oxides*

A large number of nanostructured vanadium oxides have been described during the past few years. They are synthesized via the hydrothermal treatment of aqueous solutions of V(V) precursors. Their

morphology is usually related to the layered structure of orthorhombic $V_2O_5$. Therefore 1D and 2D structures such as nanowires, nanofibres, nanorods, nanoribbons, nanobelts or nanosheets are typically reported in the literature. Temperature and pH appear to be the main parameters to control the morphology of these $V_2O_5$ based nanomaterials [19].

Heating $V_2O_5$ with TMAOH for instance leads to different layered compounds depending on pH [14]. Ribbon-like (TMA)[$V_8O_{20}$] particles are obtained at pH 3. They exhibit a 2D structure made of chains of edge-sharing [$VO_6$] octahedra joined together by corners to form [$V_8O_{20}$] sheets. Plate-like (TMA)[$V_4O_{10}$] particles are obtained at pH 6. Oxide layers are made up of double chains of edge and corner sharing [$VO_5$] square pyramids linked together by corners. In both cases, the structure is close to that of orthorhombic $V_2O_5$ and the main difference between both polyvanadates is the shape of the particles. Their width increases with pH, platelets are formed at pH 6 and ribbons at pH 3. This could be explained by looking at the structure of the hydrolyzed molecular precursors (Figure3). Around pH 3, the main molecular precursor (h = 5) should be $[VO(OH)_3(OH_2)_2]^0$. Olation reactions along V-$OH_2$ bonds are faster than oxolation reactions along V-OH bonds, leading to the anisotropic growth of (TMA)[$V_8O_{20}$] nanobelts or nanoribbons. The neutral precursor undergoes deprotonation when pH increases giving the anionic molecular species $[VO(OH)_4(OH_2)]^-$ around pH 6. Only oxolation reactions then occur in the *xy* plane along the four equivalent V-OH bonds leading to plate-like (TMA)[$V_4O_{10}$] particles that exhibit a truly 2D structure [40]. Above pH≈6, $V^{5+}$ ions become tetrahedrally coordinated and the resulting polyoxovanadate (TMA)[$V_3O_7$] obtained at pH 8 is a truly 2D oxide with $V_3O_7$ layers made of zig-zag chains of edge-sharing [$V^{4+}O_5$] square pyramids connected by corner-sharing [$V^{5+}O_4$] tetrahedra [41].

In all cases, large alkylammonium cations are just intercalated between the oxide layers. Some reduction occurs during the thermal treatment leading to mixed valence compounds that contain both $V^{5+}$ and $V^{4+}$ ions. The number of reduced vanadium ions increases with pH. The ratio $V^{4+}/V^{5+}$ = 1/7 at pH 3, 1/3 at pH 6 and 2 at pH 8 [15].

A large variety of polyoxovanadates exhibiting 1D or 2D structures have been reported during the past decade. As a general rule, they progressively turn from 1D to 2D as pH increases. As shown just before, this should result from the deprotonation of the fourth water molecule in the equatorial *xy* plane. Condensation via olation progressively decreases. Depending on the experimental conditions (pH and temperature) this leads to the formation of nanowires [42-45], nanofibres [46,47], nanoribbons [48], nanorods [49-53], nanobelts [54-62] and nanosheets [63].

The case of $H_2V_3O_8$ nanobelts is especially interesting. These nanobelts are obtained via the hydrothermal treatment of $V_2O_5$ suspensions (190 °C, 24 h). A pure orthorhombic crystalline phase (JCPDS 89-0612) is obtained. According to authors, the width of $H_2V_3O_8$ nanobelts can be controlled by adjusting the pH value. It increases from 100 nm at pH 3 up to 1 μm at pH 5 [64-67].

### *4.2. Vanadium oxide nanotubes*

Vanadium oxide $VO_x$ nanotubes were discovered by R. Nesper and co-workers [5,6]. They are several μm in length and offer a typical example of multiwalls tubular structures. Their walls may contain up to 30 vanadium oxide layers, giving an outer diameter up to 100 nm. Many very good papers have been published describing their structure [68-70] and physical properties: electronic [71-74],

optical [75,76], or magnetic [77]. However the main interest for these nanotubes remains their electrochemical properties. The template organic molecules can be removed without breaking the structure of the nanotubes that remain redox-active allowing the reversible insertion of $Li^+$ ions [78-84].

VOx nanotubes are currently formed via hydrothermal syntheses (≈180 °C, few days) in the presence of long chain alkyl amines such as HDA (HexaDecyl Amine). Different precursors have been used such as vanadium pentoxide $V_2O_5$ [85,86], vanadium alkoxides $VO(OR)_3$ [68,79], vanadium oxychloride $VOCl_3$ [87], ammonium metavanadate $NH_4VO_3$ [88] or vanadium oxide gels $V_2O_5$,$nH_2O$ [89,90]. In all cases, layered vanadium oxides are formed in the aqueous solution that then roll up into nanotubes [91,92]. A mixture of vanadium oxide nanotubes and unrolled vanadium oxide sheets can be observed during the hydothermal treatment, confirming the link between nanotubes and exfoliated lamellar intermediates [93]. The number of plate-like particles progressively decreases with time while more nanotubes are formed and only nanotubes are observed after few days (Figure 7).

**Figure 7.** Formation of VOx nanotubes upon hydrothermal treatment of $V_2O_5$ gels at 180C: (a) after 8h (b) after 66h ( c) after 120 h.

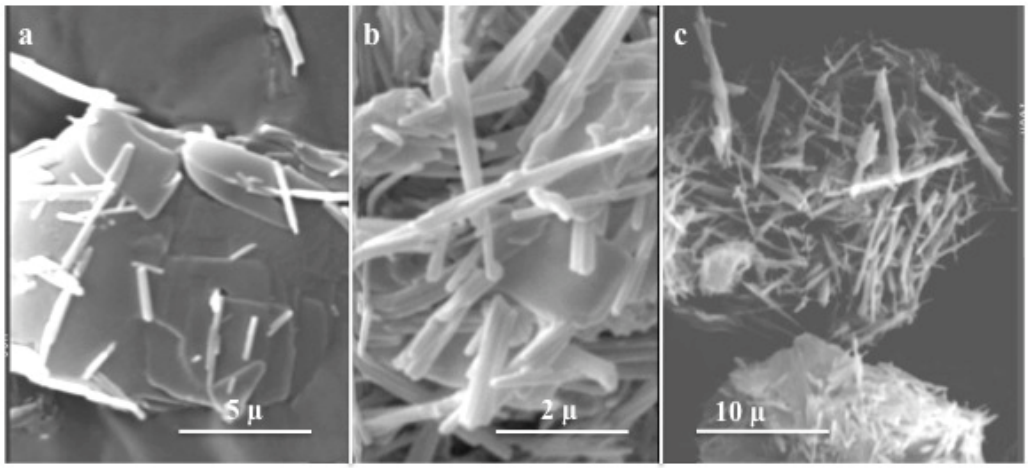


Actually two main chemical processes seem to be involved in the formation of VOx nanotubes, namely the intercalation of organic molecules between the oxide layers and the reduction of $V^{5+}$ ions.

Vanadium oxide is known to be a typical layered material. A wide range of molecular species can be intercalated between the oxide layers. The basal distance increases upon intercalation decreasing the interactions between oxide layers. A swelling process is even observed with vanadium pentoxide xerogels leading to the formation of colloidal solutions made of exfoliated $V_2O_5$ layers dispersed in water [22,93]. These oxide layers can then behave almost freely and roll up into curved structures such as nanorods, nanotubes or nanoscrolls [92,94-98].

Intercalation appears to be an important step during the formation of nanotubes. Before hydrothermal treatment, $V_2O_5$ and alkylamine mixtures have to be aged at room temperature in order to induce the intercalation process [5,68]. The size of intercalated organic molecules seems also to be important to decrease interaction between oxide layers. VOx nanotubes are obtained in the presence of long chain alkyl amines while smaller amines do not lead to the same morphology [99]. Vanadium oxide nanotubes about 120 nm in diameter are observed in the $V_2O_5$-HDA system while only nanorods

(diameter ≈ 20 nm) are formed with $V_2O_5$-EtOH **[**100**]**. It has to be pointed out that these intercalated amines can be exchanged with metal cations in the solution **[**101].

Organic molecules also favor the reduction of the oxide as shown by the color of the sample that turns from orange to green and black. This leads to the formation of a mixed valence compound that contains both $V^{5+}$ and $V^{4+}$ ions (about 50%) [102**]**. Actually, VOx nanotubes can also be obtained via the oxidation od $V^{4+}$ solutions **[**103**]**. Reduced $V^{4+}$ ions are much bigger than $V^{5+}$ ($r_{V4+}$ = 0.85 Å, $r_{V5+}$ = 0.49 Å). This can cause a significant degree of stress favoring the curvature of the oxide layers. Moreover, temperature favors the formation of tetrahedral [$VO_4$] vanadium species. It has been shown that the structure of these nanotubes is close to that of $BaV_7O_{16}$. It is made of two sheets of [$VO_5$] square pyramids pointing in opposite directions and connected by [$V^{5+}O_4$] tetrahedra [104]. These tetrahedra prevent electron delocalization all over the sample. A strong electron-phonon coupling is observed leading to the local distortion of $V^{4+}$ sites with the formation of small polarons [105].

### *4.3. Nanostructured oxides*

The hydrothermal synthesis of nanostructured vanadium oxides currently leads to 1D material such as nanotubes, nanorods, nanowires or nanobelts. However one further step could be obtained via the self assembling of these 1D structures into curved structures such as spheres, flower-like or nano urchins.

$V_2O_5$ nanorods for instance lead to the formation of ellipse-like macro-plates in which they lie parallel or perpendicular to each other [106]. Vanadium oxide bundles have been obtained via the sonication of $V_2O_5$-$H_2O$ suspensions. These spindle-like $V_2O_5$ bundles are made of several tens of 1D nanoparticles (nanowires or nanorods), with diameters 30-50 nm and lengths of 3-7 μm. Ultrasounds induce the dispersion of the oxide layers than can roll up into wires or rods and then self-assemble side-by-side into bundles [107,108]. Foreign ions such as $Co^{2+}$ ions have been shown to be able to behave as nucleation centers. They lead to the formation of bundle-like $V_2O_5.xH_2O$ nanostructures made from nanobelts synthesized via a simple hydrothermal treatment of $V_2O_5$ and $H_2O_2$ [109].

Hollow $V_2O_5$ microspheres have been obtained via the self-assembly of nanorods [110]. These nanorods about 200 nm in diameter and up to 2 μm long are formed when vanadium acetylacetonate [$V(acac)_3$] is heated with ethylene glycol. They self-assemble into hollow microspheres in the presence of poly(vinylpyrrolidone) (PVP). Ethylene glycol has been shown to give metal oxide nanowires [111,112]. Therefore the formation of rod-like vanadium precursors could be explained via the coordination of EG giving a vanadium glycolate followed by an oligomerization reaction. PVP then behaves as a template in which vinyl groups are hydrophobic while carbonyl groups are hydrophylic, leading to the formation of micelles. Vanadium oxide microspheres, made of closely packed particles and radially aligned rods, are also formed in the presence of oxalic acid. [113-115]

Roselike nanostructured vanadium oxide films have been synthesized from water-ethanol solutions of vanadium tri-isopropoxide $VO(OPr^i)_3$, using hexadecylamine as a template. These films are obtained by drop-casting of the solution onto Si wafers. They are made of radially packed petal-like flat structures giving rise to spherical aggregates about 40 nm in diameter. These films exhibit photo-induced hydrophilic properties. They can switch reversibly between superhydrophobic and superhydrophilic under UV irradiation and dark storage respectively **[**116]. Similar roselike nanostructures have also been obtained via the thermal decomposition of ammonium vanadium sulfate

hydroxide [$NH_4V_3(OH)_6(SO_4)_2$]. This compound synthesized via the hydrothermal treatment of $NH_4VO_3$ with oxalic acid in a DMSO-$H_2O$ solvent is made of flat particles that self-assemble into a rose-like structure. A pure $V_2O_5$ phase is obtained upon calcination at 500 °C without destroying the flower morphology [117]. Such flower-like nanostructures are not limited to V(V) oxides, nanostructured reduced vanadium oxides such as $VO_2$ petaloid clusters or VOOH hollow dandelions have also been described recently [118,119].

The most amazing nanostructured vanadium oxide described during the past few years should be the spherical clusters that look like 'nano-urchins' [120,121]. They have been obtained via the hydrothermal treatment of an ethanolic solution of vanadium tri-isopropoxide and alkyl amines. A layered compound is first formed with alkyl amines intercalated between the oxide layers. These oxide lamina self-organize into a fan-like laminar structure, presumably because of the presence of non intercalated free amines. They then roll up to form hollow nanotubes that can be up to several micrometers in length. The tube walls are made of vanadium oxide layers with intercalated organic surfactant molecules. The radial self-organization of $VO_x$ nanotubes leads to the formation of spherical structures that look like nano-urchins. Almost perfect scrolled layers are formed under highly reducing conditions when the amine intercalation is maximized while 'nano-urchin' structures are formed under less reducing conditions [122,123]. Amazing six-fold rotationally symmetric vanadium oxide nanostructures have been obtained from $V_2O_5$ xerogels treated with dodecanethiol. Each nanostructure is made of six spoke-like $V_6O_{11}$ platelets making an angle of about 60°. Their formation from the layered xerogel is explained via a morphotropic transition [124].

**Figure 8.** Nanostructured vanadium oxides obtained via the self-assembling of nanoparticles: a) and b) Nano-urchin from VOx nanotubes, c) and d) nanospheres from platelets hexavanadate nanoparticles $Cs_2V_6O_{16}$.

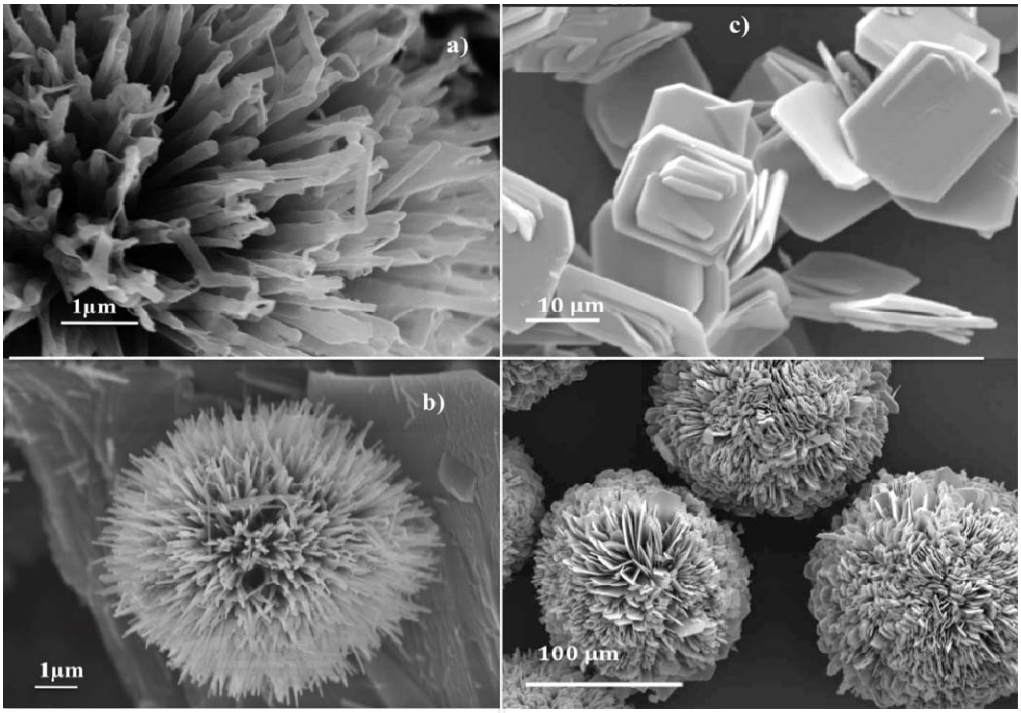

## 5. Conclusion

Nanostructured vanadium oxides have been widely studied during the past decade. Many syntheses, such as chemical vapor deposition [125] or anodic deposition, also lead to amazing morphologies [126,127]. However, most syntheses are based on the hydrothermal treatment of aqueous solutions. These nanostructured vanadium oxide based materials range from molecular polyoxovanadate clusters to nanotubes and even nano-urchins. Some strong correlations can be drawn between the molecular structure of solute precursors in the solution and the nanostructure of the resulting materials. Their analysis should lead to a better control of the synthesis of these nanostructured vanadium oxides. Temperature, pH, foreign organic or inorganic species are some of the main parameters. The structure of nano-urchins, nanotubes and nanorods for instance depends strongly on the valency of vanadium and its interactions with the organic surfactants [122,123].

Nanostructured vanadium oxide exhibits specific properties that could be used for the realisation of new devices. The role of nanostructure in improving the performance of electrodes for energy storage and conversion has been clearly demonstrated [128,129]. The electrochemical insertion of $Li^+$ ions for instance appears to be much easier and reversible into nanostructured vanadium oxides than in bulk $V_2O_5$, a property that could be exploited for lithium batteries. Open-ended multiwalled nanotubes have been shown to exhibit improved electrochemical properties. They have a high initial discharge capacity of 457 $mAh^{-1}$ and good cycling performances [79,83**]**.

Well ordered VOx nanorolls are obtained under highly reducing conditions. Their electrochemical responses are similar to those of crystalline $V_2O_5$. A significant increase in specific capacity is observed with defect-rich vanadium oxide nanorolls obtained under less reducing conditions. The association of nanoscale and atomic scale disorder appears to produce the best combination of increased specific capacity and better cyclability. Therefore, the unprecedented density of urchin's nanotubes, could open new possibilities for making lithium nano-batteries [130].

## References

1. Wang, Z.L. Nanobelts, nanowires and nanodiskettes of semiconducting oxides - from materials to nanodevices. *Adv. Mater*. **2003**, *15*, 432-436.
2. Xia, Y.; Yang, P.; Sun, Y.; Wu, Y.; Mayers, B.; Gates, B.; Yin, Y.; Kim, F.; Yan, H. One-dimensional nanostructures: synthesis, characterization and applications. *Adv. Mater*. **2003**, *15*, 353-389.
3. Bazito, F.C.; Torresi, R.M. Cathodes for lithium ion batteries: the benefit of using nanostructured materials. *J. Braz. Chem. Soc*. **2006**, *17*, 627-642.
4. Wang, Y.; Cao, G. Developments in nanostructured cathode materials for high-performance lithium-ion batteries. *Adv. Mater*. **2008**, *20*, 2251-2269.
5. Spahr, M.E.; Bitterli, P.; Nesper, R.; Muller, M.; Krumeich, F.; Nissen, H.U. Redox active nanotubes of vanadium oxide. *Angew. Chem. Int. Ed*. **1998**, *37*, 1263-1265.
6. Nesper, R.; Muhr, H.J. Nanotubes—an outstanding set of nano particles. *Chimia* **1998**, *52*, 571-578.

7. Schoiswohl, J.; Surnev, S.; Netzer, F.P.; Kresse, G. Vanadium oxide nanostructure: from zero to three-dimensional. *J. Phys.-Condens. Matter*. **2006**, *18*, R1-R14.
8. Wang, Y.; Cao, G. Synthesis and enhanced intercalation properties of nanostructured vanadium oxides. *Chem. Mater*. **2006**, *18*, 2787-2804.
9. Sun, D.; Kwon, C.W.; Baure, G.; Rivhman, E.; MacLean, J.; Dunn, B.; Tolbert, S.H. The relationship between nanoscale structure and electrochemical properties of vanadium oxide nanorolls. *Adv. Funct. Mate*r. **2004**, *14*, 1197-1204.
10. Lee, K.; Wang, Y.; Cao, G. Dependence of electrochemical properties of vanadium oxide films on their nano- and microstructures. *J. Phys. Chem. B* **2005**, *109*, 16700-16704.
11. Wang, Y.; Takahashi, K.; Lee, K.; Cao, G. Nanostructured vanadium oxide electrodes for enhanced lithium-ion intercalation. *Adv. Funct. Mater*. **2006**, *16*, 1133-1144.
12. Shimizu, A.; Watanabe, T.; Inagaki, M. Single-crystal study of topotactic changes between $NH_4VO_3$ and $V_2O_5$. *J. Mater. Chem*. **1994**, *4*, 1475-1478.
13. Zavalij, P.Y.; Whittingham, M.S. Structural chemistry of vanadium oxides with open frameworks. *Acta Cryst.* **1999**, *B55*, 627-663.
14. Hagrman, P.J.; Finn, R.C.; Zubieta, J. Molecular manipulation of solid state structure: influence of organic components on vanadium oxide architectures. *Solid State Sci.* **2001**, *3*, 745-474.
15. Chirayil, T.; Zavalij, P.Y.; Whittingham, M.S. Hydrothermal synthesis of vanadium oxides. *Chem. Mater*. **1998**, *10*, 2629-2640.
16. Baess, C.F.; Mesmer, R.E. *Hydrolysis of cations*; Wiley: New York, NY, USA, 1976.
17. Livage, J.; Henry, M.; Sanchez, C. Sol-gel chemistry of transition metal oxides. *Prog. Solid State Chem*. **1988**, *18*, 259-341.
18. Henry, M.; Jolivet, J.P.; Livage, J. Aqueous chemistry of metal cations: hydrolyis, condensation and complexation. *Struct. Bond.* **1992**, *77*, 154-206.
19. Livage, J. Synthesis of polyoxovanadates via chimie douce. *Coord. Chem. Reviews* **1998**, *178-180*, 999-1018.
20. Sadoc, A.; Messaoudi, S.; Furet, E.; Gautier, R.; Le Fur, E.; Le Pollès, L.; Pivan, J.Y. Structure and stability of $VO_2^+$ in aqueous solution: a car-parrinello and static *ab initio* study. *Inorg. Chem*. **2007**, *46*, 4835-4843.
21. Fratzky, D.; Götze, T.; Worzala, H.; Meisel, M. The formation of vanadyl phosphate hydrates from aqueous phase: a systematic study. *Mater. Res. Bull*. **1998**, *33*, 635-643.
22. Livage, J. Vanadium pentoxide gels. *Chem. Mater*. **1991**, *3*, 578-593.
23. Giorgetti, M.; Passerini, S.; WSmyrl, W.H. Evidence of bilayer structure in $V_2O_5$ xerogel. *Inorg. Chem*. **2000**, *39*, 1514-1517.
24. Petrov, V.; Trikalitis, P.N.; Bozin, E.S.; Billinge, S.J.; Vogt, T.; Kanatzidis, M.G. Structure of $V_2O_5.nH_2O$ xerogel solved by the atomic pair distribution function technique. *J. Am. Chem. Soc*. **2002**, *124*, 10157-10162.
25. Fontenot, C.J.; Wiench, J.W.; Schrader, G.L.; Pruski, M. $^{17}O$ MAS and 3QMAS NMR investigation of crystalline $V_2O_5$ and layered $V_2O_5.nH_2O$ gels. *J. Am. Chem. Soc*. **2002**, *124*, 8435-8444.
26. Evans, H.T. The molecular structure of the isopoly complex ion, decavanadate ($V_{10}O_{28}^{6-}$). *Inorg. Chem*. **1966**, *5*, 967-977.

27. Heath, E.; Howard, O.W. Vanadium-51 and oxygen-17 nuclear magnetic resonance study of vanadate (V) equilibria and kinetics. *J. Chem. Soc. Dalton* **1981**, 1105-1110.
28. Wery, A.S.; Gutierez-Zorrilla, J.M.; Luque, A.; Ugalde, M.; Roman, P. Phase transition in metavanadates. Polymerization of tetrakis(tert-butylammonium)-cyclo-tetrametavanadate. *Chem. Mater.* **1996**, *8*, 408-413.
29. Bouhedja, L.; Steunou, N.; Maquet, J.; Livage, J. Synthesis of polyoxovanadates from aqueous solutions. *J. Solid State Chem*. **2001**, *162*, 315-321.
30. Riou, D.; Roubeau, O.; Ferey, G. Evidence for the solid state structural transformation of the network type decavanadate into a lamellar topology. *Z. Anorg. Allg. Chem*. **1998**, *624*, 1021-1025.
31. Drezen, T.; Joubert, O.; Ganne, M.; Brohan, L. Synthesis and structure determination of a novel centered tricosahedral cluster compound related to the Müller-type structure. *J. Solid State Chem*. **1998**, *136*, 298-304.
32. Chen, Y.; Gu, X.; Peng, J.; Shi, Z.; Yu, H.; Wang, E.; Hu, N. The first discrete mixed-valence hexadecavanadate host shell cluster anions: hydrothermal synthesis, structure and characterization of $[V_{16}O_{38}Cl]^{8-}$. *Inorg. Chem. Comm*. **2004**, *7*, 705-707.
33. Klemperer, W.G.; Marquaet, T.A.; Yaghi, O.M. New directions in polyvanadate chemistry: from cages and clusters to baskets, belts, bowls and barrels. *Angew. Chem. Int. Ed*. **1992**, *31*, 49-51.
34. Müller, A.; Krickemeyer, E.; Penk, M.; Rohlfing, R.; Armatage, A.; Bögge, H. Template-controlled formation of cluster shells or a type of molecular recognition: synthesis of $[HV_{22}O_{54}(ClO_4)]^{6-}$ and $[H_2V_{18}O_{44}(N_3)]^{5}$. *Angew. Chem. Int. Ed*. **1991**, *30*, 1674-1677.
35. Müller, A.; Penk, M.; Rohlfing, R.; Krickemeyer, E.; Döring, J. Formation of a cluster sheath around a central cluster by a 'self-organization process': the mixed valence polyoxovanadate $[V_{34}O_{82}]^{10-}$. *Angew. Chem. Int. Ed*. **1991**, *30*, 588-590.
36. Müller, A.; Sessoli, R.; Krickemeyer, E.; Bögge, H.; Meyer, J.; Gatteschi, D.; Pardi, L.; Westphal, J.; Hovemeier, K.; Rohlfing, R.; Döring, J.; Hellweg, F.; Beugholt, C.; Schmidtmann, M. Polyoxovanadates: high-nuclearity spin clusters with interesting host-guest systems and different electron populations. Synthesis, spin organization, magnetochemistry, and spectroscopic studies. *Inorg. Chem*. **1997**, *36*, 5239-5250.
37. Müller, A. Induced molecule self-organization. *Nature* **1991**, *352*, 115.
38. Steunou, N.; Bouhedja, L.; Castro-Garcia, S.; Livage, J. Chemically controlled hydrothermal syntheses of vanadium oxides. *High Pressure Res.* **2001**, *20*, 55-62.
39. Rohmer, M.M.; Deveny, J.; Wiest, R.; Benard, M. *Ab initio* modeling of the endohedral reactivity of polyoxometallates: host-guest interactions in $[RCN(V_{12}O_{32}^{4-}]$ (R=H, $CH_3$, $C_6H_5$). *J. Am. Chem. Soc*.**1996**, *118*, 13007-13014.
40. Zavalij, P.Y.; Whittingham, M.S.; Boylan, E.A.; Pecharsky, V.K.; Jacobson, R.A. New structure $TMAV_4O_{10}$. *Z. Krist*. **1996**, *211*, 464.
41. Chirayil, T.G.; Boylan, E.A.; Mammak, M.; Zavalij, P.Y.; Whittingham, M.S. $NMe_4V_3O_7$: critical role of pH in hydrothermal synthesis of vanadium oxides. *Chem. Commun*. **1997**, 33-34.
42. Zhou, F.; Zhao, X.; Yuan, C.; Li, L.; Xu, H. Low-temperature hydrothermal synthesis of orthorhombic vanadium pentoxide nanowires. *Chem. Lett.* **2007**, *36*, 310.

43. Zhou, F.; Zhao, X.; Yuan, C.; Li, L. Vanadium pentoxide nanowires: hydrothermal synthesis, formation, mechanism and phase control parameters. *Cryst. Growth Des*. **2008**, *8*, 7234-727.
44. Gao, S.; Chen, Y.; Luo, H.; Jiang, L.; Ye, B.; Wei, M.; Wei, K. Single-crystal vanadium pentoxide nanowires. *J. Nanosci. Nanotechnol*. **2008**, *8*, 3500-3503.
45. Muster, J.; Kim, G.T.; Krstic, V.; Park, J.G.; Park, Y.W.; Roth, S.; Burghard, M. Electrical transport through individual vanadium pentoxide nanowires. *Adv. Mater*. **2000,** *12*, 420-424.
46. Kim, G.T.; Muster, J.; Krstic, V.; Park, J.G.; Park, Y.W.; Roth, S.; Burghard, M. Field-effect transistor made of individual $V_2O_5$ nanofibers. *Appl. Phys. Lett.* **2000**, *76*, 1875-1877.
47. Gu, G.; Schmid, M.; Chiu, P.W.; Minett, A.; Fraysse, J.; Kim, G.T.; Roth, S.; M. Kozlov, M.; Munoz, E.; Baughman, R.H. $V_2O_5$ nanofibre sheet actuators. *Nature* **2003**, *2*, 316-318.
48. Chan, C.K.; Peng, H.; Twesten, R.D.; Jarausch, K.; Zhang, F.; Cui, Y. Fast, completely reversible Li insertion in vanadium pentoxide nanoribbons. *Nano Lett.* **2007**, *7*, 490-495.
49. Pinna, N.; Willinger, W.; Weiss, K.; Urban, J.; Schlögl, R. Local structure of nanoscopic materials: $V_2O_5$ nanorods and nanowires. *Nano Lett.* **2003**, *3*, 1131-1134.
50. Pinna, N.; Wild, U.; Urban, J.; Schlögl, R. Divanadium pentoxide nanorods. *Adv. Mater.* **2003**, *15*, 329-331.
51. Takahashi, K.; Limmer, S.J.; Wang, Y.; Cao, G. Synthesis and electrochemical properties of single-crystal $V_2O_5$ nanorods arrays by templated-based electrodeposition. *J. Phys. Chem. B* **2004**, *108*, 9795-9800.
52. Pavasupree, S.; Suzuki, Y.; Kitiyanan, A.; Pivsa-Art, S.; Yoshikawa, S. Synthesis and characterization of vanadium oxides nanorods. *J. Solid State Chem*. **2005**, *18*, 2152-2158.
53. Asim, N.; Radiman, S.; Yarmo, M.A.; Banaye Golriz, M.S. Vanadium pentoxide: synthesis and characterization of nanorod and nanoparticle $V_2O_5$ using CTAB micelle solution. *Microporous Mesoporous Mat.* **2009**, *120*, 397-401.
54. Liu, J.; Wang, X.; Peng, Q.; Li, Y. Vanadium pentoxide nanobelts: highly selective and stable ethanol sensor materials. *Adv. Mater*. **2005**, *17*, 764-767.
55. Li, G.; Pang, S.; Jiang, L.; Guo, Z.; Zhang, Z. Environmentally friendly chemical route to vanadium oxide single-crystalline nanobelts as a cathode material for lithium-ion batteries. *J. Phys. Chem. B* **2006**, *110*, 9383-9386.
56. Li, B.; Xu, Y.; Rong, G.; Jing, M.; Xie, Y. Vanadium pentoxide nanobelts and nanorolls: from controllable synthesis to investigation of their electrochemical properties and photocatalytic activities. *Nantechnology* **2006**, *17*, 2560-2566.
57. Ren, X.; Jiang, Y.; Zhang, P.; Liu, J.; Zhang, Q. Preparation and electrochemical properties of $V_2O_5$ submicron-belts sythesized by a sol-gel $H_2O_2$ route. *J. Sol-Gel Sci. Technol*. **2009**, *51*, 133-138.
58. Lu, C.; Ding, Z.; Lipson, R.H. A new chimie douce approach to crystalline vanadium pentoxide nanobelts. *J. Mater. Chem*. **2009**, *19*, 6512-6515.
59. Yu, J.; Liu, S.; Cheng, B.; Xiong, J.; Yu, Y.; Wang, J. Polymer-directed large-scale synthesis of sigle-crystal vanadium oxide nanobelts. *Mater. Chem. Phys*. **2006**, *95*, 206-210.
60. Mai, L.Q.; Lao, C.S.; Hu, B.; Zhou, J.; Qi, Y.Y.; Chen, W.; Gu, E.D.; Wang, Z.L. Synthesis and electrical transport of single-crystal $NH_4V_3O_8$ nanobelts. *J. Phys. Chem. B* **2006**, *110*, 18138-18141.

61. Reddy, C.V.; Wei, J.; Yao, Q.Z.; Rong, Z.D.; Wen, C.; Mho, S.I.; Kalluru, T.R. Cathodic performance of ($V_2O_5$+PEG) nanobelts for Li ion rechargeable battery. *J. Power Sources* **2007**, *166*, 244-249.
62. Subba Reddy, C.V.; Mho, S.I.; Kalluru, R.R.; Williams, Q.L. Hydrothermal synthesis of hydrated vanadium oxide nanobelts using poly(ethylene oxide) as a template. *J. Power Sources* **2008**, *179*, 854-857.
63. Pang, S.; Li, G.; Zhang, Z. Synthesis of polyaniline-vanadium oxide nanocomposite nanosheets. *Macromol. Rapid Commun.* **2005**, *26*, 1262-1265.
64. Li, G.C.; Pang, S.P.; Wang Z.B.; Peng, H.R.; Zhang, Z.K. Synthesis of $H_2V_3O_8$ single-crystal nanobelts. *Eur. J. Inorg. Chem*. **2005**, 2060-2063.
65. Chang, K.H.; Hu, C.C. $H_2V_3O_8$ single-crystal nanobelts: Hydrothermal preparation and formation mechanism. *Acta Mater.* **2007**, *55*, 6192-6197.
66. Qiao, H.; Zhu, X.; Zheng, Z.; Liu, L.; Zhang, L. Synthesis of $V_3O_7.H_2O$ nanobelts as cathode materials for lithium-ion batteries. *Electrochem. Commun*. **2006**, *8*, 21-26.
67. Gao, S.; Chen, Z.; Wei, M.; Wei, K.; Zhou, H. Single crystal nanobelts of $V_3O_7.H_2O$: a lithium intercalation host with a large capacity. *Electrochim. Acta* **2009**, *54*, 1115-1118.
68. Krumeich, F.; Muhr, H.J.; Niederberger, M.; Bieri, F.; Schnyder, B.; Nesper, R. Morphology and topochemical rections of novel vanadium oxide nanotubes. *J. Am. Chem. Soc*. **1999**, *121*, 8324-8328.
69. Avansi Jr., W.; Ribeiro, C.; Leite, E.; V.R. Mastelaro, V.R. Vanadium pentoxide nanostructures: an effective control of morphology and crystal structure in hydrothermal conditions. *Cryst. Growth Des.* **2009**, *9*, 3626-3631.
70. Muhr, H.J.; Krumeich, F.; Schönholzer, U.P.; Bieri, F.; Niederberger, M.; L.J. Gauckler, L.J.; Nesper, R. Vanadium oxide nanotubes - a new flexible vanadate nanophase. *Adv. Mater.* **2000**, *12*, 231-234.
71. Ivanovskaya, V.V.; Enyashin, A.N.; Sofronov, A.A.; Makurin, Y.N.; Medvedeva, N.I.; Ivanovskii, A.L. Electronic properties of single-walled $V_2O_5$ nanotubes. *Solid State Comm*. **2003**, *126*, 489-493.
72. Enyashin, A.N.; Ivanovskzya, V.V.; Makurin, Y.N.; Ivanovskii, A.L. Electronic band structure of scroll-like divanadium pentoxide nanotubes. *Phys. Letters A* **2004**, *326*, 152-156.
73. Sipos, B.; Duchamp, M.; Magrez, A.; Forro, L.; Barisic, N.; A. Kis, A.; Seo, J.W.; F. Bien, F.; Krumeich, F.; Nesper, R.; Patzke, G.R. Mechanical and electronic properties of vanadium oxide nanotubes. *J. Appl. Phys*. **2009**, *105*, 074317:1-074317:5.
74. Cao, J.; Musfeldt, J.L.; Mazumdar, S.; Chernova, N.A.; Whittingham, M.S. Pinned low-energy elctronic excitation in metal-exchange vanadium oxide nanoscrolls. *Nano Letters*, **2007**, *7*, 2351-2355.
75. Liu, X.; Täschner, C.; Leonhardt, A.; Rümmeli, M.H.; Pichler, T.; Gemming, T.; B. Büchner, B.; Knupfer, M. Structural, optical and electronic properties of vanadium oxide nanotubes. *Phys. Rev. B* **2005**, *72*, 115407:1-115407:5.
76. Webster, S.; Czerw, R.; Nesper, R.; DiMaio, J.; Xu, J.F.; Ballato, J.; Carroll, D.L. Optical properties of vanadium oxide nanotubes. *J. Nanosci. Nanotech.* **2004**, *4*, 260-264.

77. Vavilova, E.; Herllmann, I.; Kataev, V.; Täschner, C.; Büchner, B.; Klingeler, R. Magnetic properties of vanadium oxide nanotubes probed by static magnetization and $^{51}V$ NMR. *Phys. Rev. B* **2006**, *73*, 1-7.
78. Spahr, M.E.; Stoschitzki-Bitterli, P.; Nesper, R.; Haas, O.; Novak, P. Vanadium oxide nanotubes, a new nanostructured redox-active material for the electrochemical insertion of lithium. *J. Electrochem. Soc*. **1999**, *146*, 2780-2783.
79. Sun, D.; Kwon, C.W.. Baure, G.; Richman, E.; MacLean, J.; Dunn, B.; Tolbert, S.H. The relationship between nanoscale structure and electrochemical properties of vanadium oxide nanorolls. *Adv. Funct. Mater*. **2004**, *14*, 1197-1204.
80. Li, H.X.; Jiao, L.F.; Yuan, H.T.; Zhang, M.; Guo, J.; Wang, L.Q.; Zhao, M.; Wang, Y.M. Factors affecting the electrochemical performance of vanadium oxide nanotube cathode materials. *Electrochem. Comm*. **2006**, *8*, 1693-1698.
81. Nordlinder, S.; Nyholm, L.; Gustafsson, T.; Edström, K. Lithium insertion into vanadium oxide nanotubes: electrochemical and structural aspects. *Chem. Mater*. **2006**, *18*, 495-503.
82. Mohan, V.M.; Hu, B.; Qiu, W.; Chen, W. Synthesis, stuctural and electrochemical performane of $V_2O_5$ nanotubes as cathode material for lithium battery. *J. Appl. Electrochem*. **2009**, *39*, 2001-2006.
83. Cui, C.J.; Wu, G.M.; Shen, J.; Zhou, B.; Zhang, Z.H.; Yang, H.Y.; She, S.F. Synthesis and electrochemical performance of lithium vanadium oxide nanotubes as cathodes for rechargeable lithium-ion batteries. *Electrochim. Acta* **2010**, *55*, 2536-2541.
84. Patzke, G.R.; Krumeich, F.; R. Nesper, R. Oxidic nanotubes and nanorods - anisotropic modules for a future nanotechnology. *Angew. Chem. Int. Ed*. **2002**, *41*, 2446-2461.
85. Sharma, S.; Thomas, J.; Ramanan, A.; Panthöfer, M.; Jansen, M. Hydrothermal synthesis of vanadium oxide nanotubes from oxide precursors. *J. Nanosci. Nanotechn*. **2007**, *6*, 1985-1989.
86. Mai, L.; Chen, W.; Xu, Q.; Zhu, Q.; Han, C.; Peng, J. Cost-saving synthesis of vanadium oxide nanotubes. *Solid State Comm*. **2003**, *126*, 541-543.
87. Niedderberger, M.; Muhr, H.J.; Krumeich, F.; Bieri, F.; Günther, D.; Nesper, R. Low-cost synthesis of vanadium oxide nanotubes via two novel non-alkoxide routes. *Chem. Mater*. **2000**, *12*, 1995-2000.
88. Asim, N.; Radiman, S.; Yarmo, M.A.; Banaye Golriz, M.S. Vanadium pentoxide: synthesis and characterization of nanorod and nanoparticle $V_2O_5$ using CTAB micellle solution. *Microporous Mesoporous Mat.* **2009**, *120*, 397-401.
89. Chandrappa, G.T.; Steunou, N.; Cassaignon, S.; Bauvais, C.; Livage, J. Hydrothermal synthesis of vanadium oxide nanotubes from $V_2O_5$ gels. *Catal. Today* **2003**, *78*, 85-89
90. Chen, W.; Peng, J.; Mai, L.; Zhu, Q.; Xu, Q. Synthesis of vanadium oxide nanotubes from $V_2O_5$ sols. *Mater. Lett*. **2004**, *58*, 2275-2278.
91. Petkov, V.; Zavalij, P.Y.; Lutta, S.; Whittingham, M.S.; Parvanov, V.; Shastri, S. Structure beyond Bragg: study of $V_2O_5$ nanotubes. *Phys. Rev. B*, **2004**, *69*, 9085410:1-9085410:6.
92. Krumeich, F.; Muhr, H.J.; Niederberger, M.; Bieri, F.; Nesper, R. The cross-sectional structure of vanadium oxide nanotube studied by transmission electron microscopy and electron spectroscopic imaging. *Z. Anorg. Allg. Chem*. **2000**, *626*, 2208-2216.

93. Davidson, P. Vanadium pentoxide gels: from chimie douce to matière molle. *C.R. Chim.* **2010**, *13*, 142-153.
94. Chandrappa, G.T.; Steunou, N.; Cassaignon, S.; Bauvais, C.; Biswas, P.K.; Livage, J. Vanadium oxide: from gels to nanotubes. *J. Sol-Gel Sci. Techn.* **2003**, *26*, 593-596.
95. Muhr, H.J.; Schönholzer, U.P.; Bieri, F.; Niederberger, M.; Gauckler, L.J.; Nesper, R. vanadium oxide nanotubes—a new vanadate nanophase. *Adv. Mater*. **2000**, *12*, 231-234.
96. Kweon, H.; Lee, K.W.; Lee, C.E. Coexisting structural phases in a two-dimensional vanadium oxide/surfactant nanostructure. *Curr. Appl. Phys.* **2009**, *9*, 691-693.
97. Chen, W.; Mai, L.Q.; Peng, J.F.; Xu, Q.; Zhu, Q.Y. FTIR study of vanadium oxide nanotubes from lamellar structure. *J. Mater. Sci.* **2004**, *39*, 2625-2627.
98. Chen, X.; Sun, X.; Li, Y. Self-assembling vanadium oxide nanotubes by organic molecular templates. *Inorg. Chem*. **2002**, *41*, 4524-4530.
99. Sediri, F.; Gharbi, N. From crystalline $V_2O_5$ to nanostructured vanadium oxides using aromatic amines as templates. *J. Phys. Chem. Solids* **2007**, *68*, 1821-1829.
100. Grigorieva, A.V.; Goodilin, E.A.; Anikina, A.V.; Kolesnik, I.V.; Tretyakov, Y.D. Surfactants in the formation of vanadium oxide nanotubes. *Mendeleev Commun.* **2008**, *18*, 71-72.
101. Reinoso, J.M.; Muhr, H.J.; Krumeich, F.; Bieri, F.; Nesper, R. Controlled uptake and release of metal cations by vanadium oxide nanotube. *Helv. Chim. Acta* **2000**, *83*, 1724-1733.
102. Corr, S.A.; Grossman, M.; Furman, J.D.; Melot, B.C.; Cheetham, A.K.; Heier, K.R.; Seshadri, R. Controlled reduction of vanadium oxide nanoscrolls: crystal structure, morphology and electrical properties. *Chem. Mater*. **2008**, *20*, 6396-6404.
103. Vera-Robles, L.I.; Campero, A. A novel approach to vanadium oxide nanotubes by oxidation of $V^{4+}$ species. *J. Phys. Chem. C* **2008**, *112*, 19930-19933.
104. Wörle, M.; Krumeich, F.; Bieri, F.; Muhr, H.J.; Nesper, R. Flexible $V_7O_{16}$ layers as the common structural element of vanadium oxide nanotubes and a new crystalline vanadate. *Z. anorg. allg. Chem*. **2002**, *628*, 2778-2784.
105. Sanchez, C.; Babonneau, F.; Morineau, R.; Livage, J.; Bullot, J. Semiconducting properties of $V_2O_5$ gels. *Phil. Mag. B* **1983**, *47*, 279-290.
106. Zhou, Y.; Qiu, Z.; Lü, M.; Zhang, A.; Ma, Q. Preparation and characterization of $V_2O_5$ macro-plates. *Mater. Lett.* **2007**, *61*, 4073-4075.
107. Taufiq-Yap,Y.H.; Wong, Y.C.; Zainal, Z.; Hussein, M.Z. Synthesis of self-assembled nanorod vanadium oxide bundles by sonochemical treatment. *J. Nat. Gas Chem*. **2009**, *18*, 312-318.
108. Mao, C.J.; Pan, H.C.; Wu, X.C.; Zhu, J.J.; Chen, H.Y. Sonochemical route for self-assembled $V_2O_5$ bundles with spindle-like morphology and their novel application in serum albumin sensing. *J. Phys. Chem. B* **2006**, *110*, 14709-14713.
109. Li, G.; Jiang, L.; Peng, H. A simple route to $V_2O_5.xH_2O$ bundle-like nanostructures. *Mater. Lett.* **2007**, *61*, 4070-4072.
110. Cao, A.M.; Hu, J.S.; Liang, H.P.; Wan, L.J. Self-assembled vanadium pentoxide ($V_2O_5$) hollow microspheres from nanorods and their application in lithium-ion batteries. *Angew. Chem. Int. Ed*. **2005**, *44*, 4391-4395.

111. Weeks, C.; Song, Y.; Suzuki, M.; Chernova, N.A.; Zavalij, P.Y.; Whittingham, M.S. The one dimensional chain structure of vanadyl glycolate and vanadyl acetate. *J. Mater. Chem*. **2003**, *13*, 1420-1423.
112. Jiang, X.; Wang, Y.; Herrivcks, T.; Xia, Y. Ethylene glycol-mediated synthesis of metal oxide nanowires, *J. Mater. Chem*. **2004**, *14*, 695-703.
113. Feng, C.Q.; Wang, S.Y.; Zeng, R.; Guo, Z.P.; Konstantinov, K.; Liu, H.K. Synthesis of spherical porous vanadium pentoxide and its electrochemical properties. *J. Power Sources* **2008**, *184*, 485-488.
114. Chen, Y.; Liu, H.; Ye, W.L. Preparation and electrochemical properties of submicron spherical V2O5 as cathode material for lithium batteries. *Scripta Mater.* **2008**, *59*, 372-375.
115. Fei, H.L.; Zhou, H.J.; Wang, J.G.; Sun, P.C.; Ding, D.T.; Chen, T.H. Synthesis of hollow $V_2O_5$ microspheres and application to photocatalysis. *Solid State Sci.* **2008**, *10*, 1276-1284.
116. Lim, H.S.; Kwak, D.; Lee, D.Y.; Goo, S.; Cho, K. UV-driven reversible switching of a roselike vanadium oxide film between superhydrophobicity and superhydrophilicity. *J. Am. Chem. Soc*. **2007**, *129*, 4128-4129.
117. Fei, H.L.; Zhou, H.J.; Wang, J.G.; Sun, P.C.; Ding, D.T.; Chen, T.H. Synthesis of $V_2O_5$ micro-architectures via *in situ* generation of single-crystalline nanoparticles. *Solid State Sci.* **2009**, *11*, 102-107.
118. Liu, X.; Huang, C.V.; Yi, S.; Xie, G.; Li, H.; Luo, Y. A new solvothermal method of preparing $VO_2$ nanosheets and petaloid clusters. *Solid State Comm*. **2007**, *144*, 259-263.
119. Wu, C.; Xie, Y.; Lei, L.; Hu, S.; OuYang, C. Synthesis of new-phased VOOH 'dandelions' and their application in lithium-ion batteries. *Adv. Mater*. **2006**, *18*, 1727-1732.
120. O'Dwyer, C.; Navas, D.; Lavayen, V.; Benavente, E.; Santa Ana, M.A.; G. Gonzalez, G.; Newcomb, S.B.; Sotomayor Torres, C.M. Nano-urchin: the formation and structure of high-density spherical clusters of vanadium oxide nanotubes. *Chem. Mater*. **2006**, *18*, 3016-3022.
121. Lavayen, V.; O'Dwyer, C.; Santa Ana, M.A.; Newcomb, S.B.; Benavente, E.; Gonzalez, G.; Sotomayor Torres, C.M. Comparative structural-vibrational study of nano-urchin and nanorods of vanadium oxide. *Phys. Stat. Sol. (b)* **2006**, *13*, 3285-3289.
122. O'Dwyer, C.; Lavayen, V.; Newcomb, S.B.; Santa Ana, M.A.; E. Benavente, E.; Gonzàlez, G.; Sotomayor Torres, C.M. Vanadate conformation variations in vanadium pentoxide nanostructures. *J. Electrochem. Soc*. **2007**, *154*, K29-K35.
123. O'Dwyer, C.; Lavayen, V.; Tanner, D.A.; Newcomb, S.B.; Benavente, E.; Gonzales, G.; Clivia, C.; Sotomayor Torres, M. Reduced surfactant uptake in three dimensional assemblies of VOx nanotube improve reversible $Li^+$ intercalation and charge capacity. *Adv. Funct. Mater.* **2009**, *19*, 1-10.
124. O'Dwyer, C.; Lavayen, V.; Fuenzalida, D.; Newcomb, S.B.; Sant Ana, M.A; Benavente, E.; Gonzalez, G.; Sotomayor Torres, C.M. Six-fold rotationally symmetric vanadium oxide nanostructures by a morphotropic phase transition. *Phys. Stat. Sol. (b)* **2007**, *244*, 4157-4160.
125. Su, Q.; Huang, C.K.; Wang, Y.; Fan, Y.C.; Lu, B.A.; Lan, W.; Wang, Y.Y.; Liu, X.Q. Formation of vanadium oxides with various morphologies by chemical vapor deposition. *J. Alloys Compounds* **2009**, *475*, 518-523.

126. Hu, C.C.; Huang, C.M.; Chang, K.H. Anodic deposition of porous vanadium oxide network with high power characteristics for pseudocapacitors. *J. Power Sources* **2008**, 185, 1594-1597.
127. Hu, Chi-Chang; Chang, Kuo-Hsin; Huang, Chao-Ming; Li, Jing-Mei. Anodic deposition of vanadium oxide for thermal-induced growth of vanadium oxide nanowires, *J. Electrochem. Soc*. **2009**, *156*, D485-D489.
128. Arico, A.S.; Bruce, P.; Scrosati, B.; Tarascon, J.M.; Van Schalkwijk, W. Nanostructured materials for advanced energy conversion and storage devices. *Nat. Mater.* **2005**, *4*, 366-377.
129. Centi, G.; Perathoner, S. The role of nanostructure in improving the performance of electrodes for energy storage and conversion. *Eur. J. Inorg. Chem*. **2009**, 3851-3878.
130. O'Dwyer, C.; Lavayen, V.; Santa, M.A.; Benavente, E.; Gonzàlez, G.; Torres, C.M.S. Anisotropic vanadium oxide nanostructured host matrices for lithium ion intercalation. *Res. Lett. Phys. Chem.* **2007**, 32528-32533.